22nd Australasian Fluid Mechanics Conference AFMC2020
Brisbane, Australia, 6–10 December 2020
DOI: 10.14264/uql.2020.xxYY

Hydrodynamic simulation of submarine far field flow

C. Chisholm[1], B. Nugoroho[1], Kevin[1], and R. C. Chin[2]

[1] Deptartment of Mechanical Engineering
University of Melbourne, Parkville, Victoria, 3010, Australia

[2] School of Mechanical Engineering
University of Adelaide, Adelaide, South Australia, 5005, Australia

Abstract

A computational study on assessing the flow from a generic fully appended DARPA SUBOFF submarine model is reported. In this study, we conduct Reynolds Averaged Navier-Stokes (RANS) simulation at $Re_L = 1.0 \times 10^6$, based on free stream velocity and the length of the hull. Care has been taken to eliminate confinement effects due to the computational domain and to capture essential flow features with sufficient grid resolution. The flow in the vicinity of the model is validated against the available data from the literature as a baseline case. The length of the simulated domain is relatively long allowing us to investigate the wake generated and its associated turbulence statistics up to 36 submarine diameters downstream of the model. We have found that the mean streamwise velocity approaches self-similarity and a power-law relationship that characterises the wake can be obtained. The turbulent kinetic energy, however, continues to evolve long into the wake, despite this there is a strong trend towards self-similarity that has not previously been observed in experiments or simulations of such a model.

Keywords
RANS; SUBOFF DARPA submarine; far-field flow, turbulent wakes.

Introduction

The wakes generated by asymmetric and streamlined bodies at high Reynolds number have been the subject of many experimental and numerical studies in the past few decades. They have important relevances to many engineering applications, for instance the optimisation of underwater vehicle design such as submarines. The study of wake flows at high Reynolds number is known to be experimentally and computationally demanding, due to their long development length and broad range of spatial scales. For this reason many previous numerical studies of generic submarine models have focused on the flow in the close vicinity of the surface (i.e. the near and intermediary wake regions) [9, 1]. Townsend [11] hypothesised that far wake (such those behind submarines) would become self-similarity and independent of Reynolds number. For a far-field wake the streamwise mean velocity and turbulent flow quantities in wakes can be entirely characterised by maximum velocity defect u_0 and half wake width l_0, the distance from the centerline to the point at which the velocity defect is $u_0/2$ [5] (see figure 1 for the illustration of wake flow behind an axisymmetric body such as a submarine).

Many recent wake flow studies have been conducted on the publicly available DARPA SUBOFF body [3, 4]. Jiménez et. al. [6] surveyed the early near wake of an appended (with fins on stern) DARPA SUBOFF at Reynolds number range $Re_L = U_\infty L/\nu = 0.49 \times 10^6$ - 1.8×10^6 using hot-wire anemometry and Pitot tube. Their study is followed by Jiménez et. al. [5], where they conducted experiments on an idealised (without appendages) DARPA SUBOFF submarine model at Reynolds numbers ranging from 1.1×10^6 to 67×10^6, up to $15D$ (15 times of the submarine model diameters) downstream from the stern in the mid-plane. Despite the relatively far measurement location of $15D$, Jiménez et. al. [5] were unable to capture the self similarity of the streamwise turbulence intensity (or turbulent kinetic energy) for all ranges of Reynolds number. Posa et. al. [10] performed wall-resolved Large Eddy Simulation (LES) of appended DARPA SUBOFF (with fins and sail) at a condition similar to the experiments of Jiménez et. al. [5], with $Re_L = 1.2 \times 10^6$ and computational domain up to $9D$ downstream of the stern tail. Their recorded turbulent intensities were not found to exhibit self-similarity in the range of their simulated domain. The study by Posa et. al. [10] is further extended by Kumar and Mahesh [7], where they simulated an idealised DARPA SUBOFF at $Re_L = 1.2 \times 10^6$ and longer computational domain (up to $17.2D$ of the stern tail). Despite a longer computational domain, the axisymmetric wake shows no self-similarity in the streamwise turbulence intensities.These experiment and numerical results show the difficulty in conducting far field flow studies of a submarine.

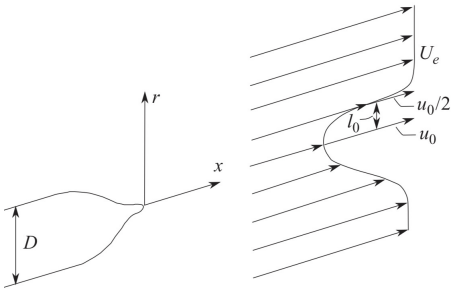

Figure 1. A schematic of a wake profile, with labels of velocity at the edge of the wake U_e, maximum velocity defect u_0, and half wake width l_0 (image is taken from Jiménez et.al. [5]).

The difficulty in recording self similarity of turbulent wake in DARPA SUBOFF, particularly for the streamwise turbulence intensity or turbulent kinetic energy has raised plenty of questions with regards of how far downstream we should observe the far field flow. In this report we conduct a Reynolds-Averaged Navier Stokes (RANS) simulation of a fully appended DARPA SUBOFF at $Re_L = 1.0 \times 10^6$ (matching many of the experimental and simulation Reynolds number), and investigated the wake up to 36D downstream of the stern tail. This computational domain is significantly longer than that of Jiménez et. al. [5] experiment and Kumar and Mahesh [7] LES.

Simulation details

We conducted a RANS simulation of a fully appended generic submarine model using the open-source computational fluid dynamics (CFD) solver OpenFoam. The software is hosted and run through The University of Melbourne's Spartan HPC (High Performing Computer) system [8]. The inlet velocity U_∞ is as-

sumed to have a constant nominal turbulence intensity of 1%. and the mean flow is assumed to be stationary.

In this study we employed the $k-\omega$ shear Stress Transport (SST) model that has been known to produce results with good agreement to experiments in a wide range of aeronautics applications [2]. The mesh used for this study consist of 20.4 Million cells after conducting a grid sensitivity study. A wall-function is applied in the near-wall region, which is a blended function of the viscous and logarithmic laws.

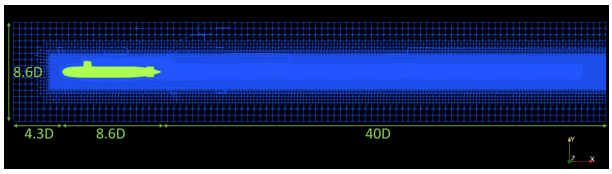

Figure 2. Computational domain of the current study.

Figure 2 shows the computational domain of the current study, with domain height of $8.6D$ and total length of $\approx 53D$, in which $40D$ is the distance between stern tail to the end of computational domain. Note the refinement region around the submarine and the wake region. The level of mesh refinement was chosen to accurately resolve the integral length scales. The inflow is located at $x/D = -4.3$ from the nose of the hull, and lateral boundaries placed at $y/D = z/D = 4.3$ from the submarine centreline.

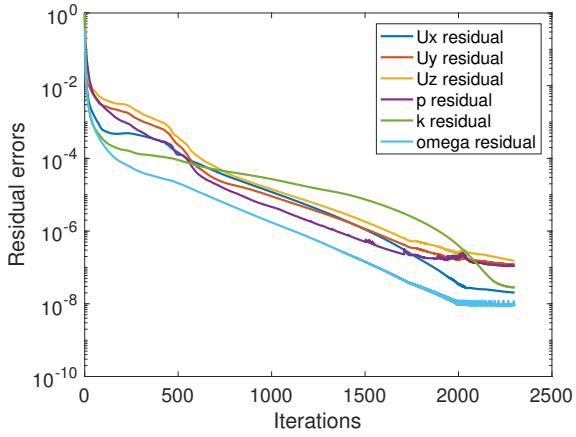

Figure 3. Normalised residuals of solution variables

To obtain a converged simulation, care was taken to ensure that the residual data from the solver log file are low. Figure 3 shows that all residuals component converged to values well below 10^{-6}, verifying that (i) boundary and initial conditions are well-posed (ii) the mesh is of sufficient quality (iii) discretization schemes and under-relaxation factors have been correctly specified.

Validation

To validate our RANS simulation, we compare the pressure distribution (Figure 4) along the submarine model and its associated skin-friction coefficient (Figure 5) with literature data. The pressure coefficient C_p and the skin-friction coefficient C_f is defined as:

$$C_p = \frac{p - p_\infty}{1/2\rho U_\infty^2}, C_f = \frac{\tau_w}{1/2\rho U_\infty^2}, \quad (1)$$

where p_∞ is the free-stream static pressure, $1/2\rho U_\infty^2$ is the dynamic pressure, ρ is the fluid density, U_∞ is free stream velocity, and τ_w is the wall shear stress.

The present results agree very well with the wall-resolved LES of Posa et al.[10] and the experimental measurement of Jiménez et. al. [5] and Huang et al. [4]. Posa et al. [10] noted that the offset between their calculated Cp and Jiménez et. al. [5] is likely due to the wind tunnel having much higher blockage than their computational domain ($\approx 5.7\%$ vs 1.4%) - for the present work the blockage is estimated to be 1.05%.

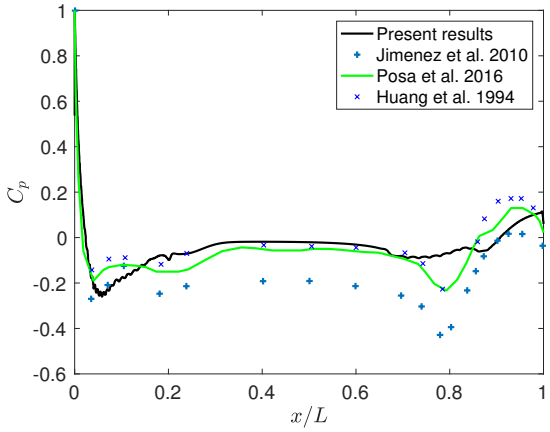

Figure 4. Coefficient of Pressure along surface of submarine (away from the influence of appendages)

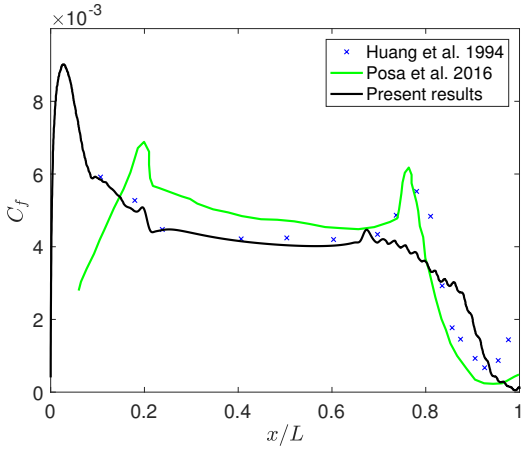

Figure 5. Skin-Friction Coefficient along surface of submarine (away from the influence of appendages)

The skin-friction coefficient C_f between our results and Posa et al.[10] in figure 5 is slightly different, particularly at the bow ($x/L \approx 0$ to 0.15) and stern ($x/L \approx 0.75$ to 1.0). We believe that this is caused by the slight differences in the submarine geometry. Figure 6 shows the comparison between our geometry (black line) and Posa et al.[10] (dotted red) geometry. Our DARPA SUBOFF submarine model has a bow with much higher curvature: being more like a sphere, while their bow is more tapered and streamlined - this explains the higher peak of C_f we calculated and also the earlier peak. Also our stern has a steady convex curvature, but ends abruptly - causing the flow to separate (note the near zero wall shear stress at the tail), whereas theirs starts with higher curvature, hence has a stronger adverse pressure gradient and sharper decrease in skin friction,

but also transitions from convex to concave - decelerating and then accelerating the flow.

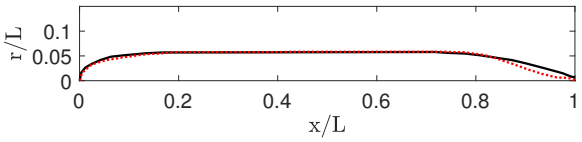

Figure 6. Comparison of hull geometry on a half plane away from any appendages. The black line is our current model outline and the dotted red lines is from Posa et al.[10].

Results

Mean velocity

Figure 7 shows the mean streamwise velocity contours along the surface and in the near wake of the submarine. The velocity has been normalised by 99% of free stream velocity U_∞ for ease to visualise the boundary layer thickness. The thick developing boundary layer due to the adverse pressure gradient on the stern and complex interaction between the boundary layer and stern appendages (junction flows) are the dominant features of the near wake, although the turbulent structures and lack of momentum in the wake of the sail also have an effect to a lesser extent. The footprint of the sail is also clearly observed in the figure.

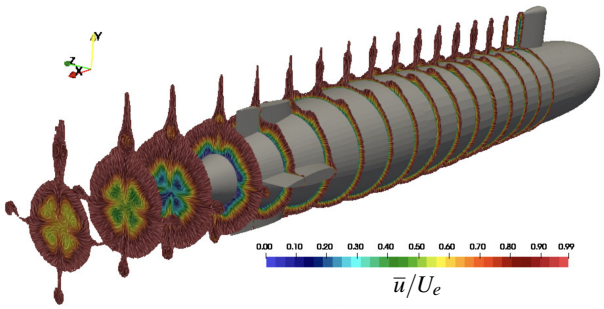

Figure 7. Scaled streamwise velocity contours at various streamwise locations.

Figure 8 illustrates the mean velocity profiles on the plane $z = 0$ (in line with the sail), non-dimensionalised by the local free-stream velocity, at locations $x = 6D$ to $36D$ downstream of the stern of the tail. The plot clearly shows that the wake strength decreases rapidly with streamwise distance as expected. A similar behaviour has been reported by Jiménez et. al both on the DARPA SUBOFF ideal model [5] and model with fins (with appendages) [6].

Figure 9 shows the velocity defect in similarity coordinates where all profiles from $x = 6D$ to $36D$ collapse within the region $-1 \leq y/l_o \leq 1$ (indicating self similarity). A least squares fit for the velocity defect in similarity coordinates is performed and can be described by the function:

$$f(\eta) = exp(-0.651\eta^2 - 0.115\eta^4 + 0.177\eta^6 - 0.081\eta^8) \quad (2)$$

where η is y/l_0. Note that equation 2 is slightly different from the DARPA SUBOFF (with appendages) correlation of Jiménez et. al [6], however from Figure 9 it seems that our fitting closely matches their approximation (red dashed line).

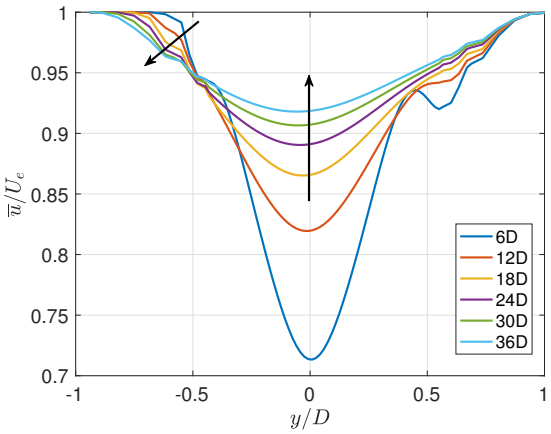

Figure 8. Mean velocity profiles $\overline{u}$ normalised by the local free-stream velocity U_e at the locations of $6D$ to $36D$ downstream of the stern of the tail. The arrows show trend of increasing streamwise distance from the stern of the tail.

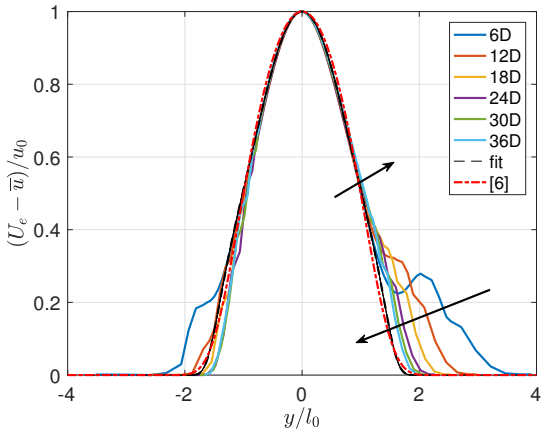

Figure 9. Velocity defects in self-similar coordinates at the locations of $6D$ to $36D$ downstream of the stern of the tail. The dashed black lines is the least squares fitting from our simulation and the dot-dashed red line is from the DARPA SUBOFF (with appendages) correlation of Jiménez et. al [6]

Turbulent kinetic energy

The turbulent kinetic energy can be defined as the half the sum of the variances of the u (streamwise), v (wall-normal), and w (spanwise) velocity components:

$$k = \frac{1}{2}\left(\overline{u'^2 + v'^2 + w'^2}\right) \quad (3)$$

The turbulent kinetic energy k at the locations of $6D$ to $36D$ downstream of the stern of the tail is shown in figure 10. Similar to the mean velocity profiles, the turbulent kinetic energy decreases with increasing streamwise distance from the stern of the tail and the profiles become more symmetric. The plot also shows that the peaks of the turbulent kinetic energy decrease monotonically with streamwise location and drift outwards due to the slow radial spreading out of the turbulent wake. Interestingly, this is not the case when the turbulent kinetic energy is plotted in similarity form (Figure 11), here the peaks at all locations in the wake are located at $y/l_0 \approx \pm 0.5$. Similar peaks are also observed on the DARPA SUBOFF with appendages LES

of Posa et al.[10].

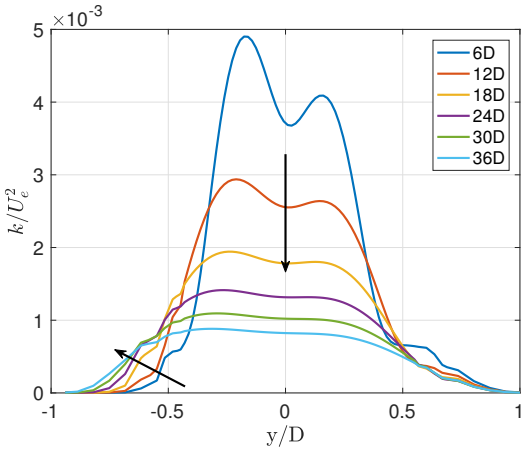

Figure 10. Distributions of the mean square turbulent kinetic energy at the locations of 6D to 36D downstream of the stern of the tail.

The turbulent kinetic energy profile in similarity form (Figure 11) do not collapse in the same fashion as the mean streamwise velocity, even at 36D downstream of the stern of the tail although they seem to approach this condition asymptotically. This is consistent with the findings of Jiménez et. al [5, 6], Posa et al.[10], and Kumar and Mahesh [7] who observed no similarity of turbulent intensities over the length of their respective domains - the longest of which extended 15 diameters downstream of the tail. If we extrapolate the trend towards collapse (i.e. fit a power law to the centerline value) the turbulent kinetic energy in the wake is estimated to achieve self similarity from $x \approx 54D$ (illustrated with dashed black line in Figure 11).

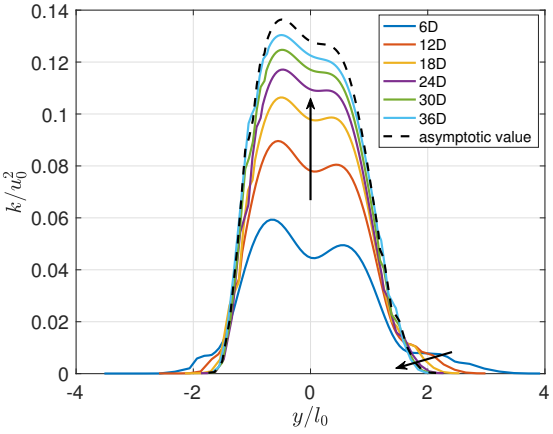

Figure 11. Turbulent kinetic energy in self-similar coordinates at the locations of 6D to 36D downstream of the stern of the tail. The dashed black lines is a power law fitting indicating the expected location where the turbulent kinetic energy would collapse.

Conclusion

In this study, we have demonstrated that RANS turbulence modelling can be applied to predict complex 3-Dimensional flows at high Reynolds number with strong adverse pressure gradients and separation, in this case the flow over a DARPA SUBOFF submarine model with appendages and its generated wake. Our results agree well with the various experimental and numerical data in the literatures. Despite having a very long downstream computational domain of 36D (more than 2$\times$ longer than literatures data), our result shows that the turbulent kinetic energy behind the submarine model is yet to achieve similarity. We estimate that the flow would reach self similarity at $x \approx 54D$, which is around 1.5 times longer than our domain.

Acknowledgement

This research was undertaken using the LIEF HPC-GPGPU Facility hosted at the University of Melbourne. This Facility was established with the assistance of LIEF Grant LE170100200

References

[1] Bhushan, S., Alam, M. F. and Walters, D. K., Evaluation of hybrid rans/les models for prediction of flow around surface combatant and suboff geometries, *Comp & Fluids*, **88**, 2013, 834–849.

[2] Brett, J., Tang, L., Hutchins, N. and Ooi, A., Computational fluid dynamics analysis of the 1303 unmanned combat air vehicle, in *17th Australiasian Fluid Mechanics Conference*, 2010.

[3] Groves, N. C., Huang, T. T. and Chang, M. S., Geometric characteristics of darpa suboffmodels, *Tech. Rep. DTRC/SHD-1298-01*, david Taylor Research Center, Bethesda, MD.

[4] Huang, T. T., Liu, H. L., Groves, N., Forlini, T., Blanton, J. and Gowing, S., Measurements of flows over an axisymmetric body with various appendages in a wind tunnel: the darpa suboff experimental program, *19th Symposium on Naval Hydrodynamics. Seoul, Korea, 23-28 August 1992, National Academy Press.*.

[5] Jiménez, J. M., Hultmark, M. and Smits, A. J., The intermediate wake of a body of revolution at high reynolds numbers, *J. Fluid Mech.*, **659**, 2010, 516?539.

[6] Jiménez, J. M., Reynolds, R. and Smits, A. J., The effects of fins on the intermediate wake of a submarine models, *J. Fluids Eng.*, **132(3)**, 2010, 031102.

[7] Kumar, P. and Mahesh, K., Large-eddy simulation of flow over an axisymmetric body of revolution, *J. Fluid Mech.*, **853**, 2018, 537–563.

[8] Lafayette, L., Sauter, G., Vu, L. and Meade, B., Spartan performance and flexibility: An hpc-cloud chimera, in *OpenStack Summit*, 2016.

[9] Pan, Y. C., Zhang, H. X. and Z, Q. D., Numerical prediction of submarine hydrodynamic coefficients using cfd simulation, *J. of Hydrodynamics*, **24**, 2012, 840–847.

[10] Posa, A. and Balaras, E., A numerical investigation of the wake of an axisymmetric body with appendages., *J. Fluid Mech.*, **792**, 2016, 470–498.

[11] Townsend, A. A., *The structure of turbulent shear Flow*, Cambridge University Press, 1956.